WETTING TESTS IN SIMPLE SHEAR CONDITIONS AND CONSTITUTIVE MODELLING

Mariagiovanna Moscariello, Sabatino Cuomo
Università degli Studi di Salerno, Italy
mamoscariello@unisa.it, scuomo@unisa.it

Yanni Chen, Giuseppe Buscarnera
Northwestern University, USA
yannichen2021@u.northwestern.edu, g-buscarnera@northwestern.edu

Sommario

The paper deals with a methodology to calibrate a constitutive model for a large database of experimental tests, which also considers the variability of the physical and mechanical soil properties. The tested material is a pyroclastic soil originated from the Somma-Vesuvius volcano. An elastoplastic strain-hardening constitutive model proposed by Buscarnera and di Prisco (2013) was used simulate its mechanical behaviour in simple shear condition in saturated or unsaturated regimes, as well as upon the transition from unsaturated to saturated. Based on the variability of the soil properties, five different confidence levels (and their boundary values) were identified for each variable. A sensitivity analysis was carried out to allow the identification of the mechanical properties which most impacted the performance of the constitutive model. An optimization procedure was adopted and a single set of constitutive parameters obtained, which provided satisfactory simulation of the hydro-mechanical simple shear soil response under several saturation condition and failure mechanisms.

1. Introduction

In landslide susceptibility analysis, a relevant issue is the proper modelling of the complex mechanisms that regulate the failure and post-failure stages. For this reason, experimental and numerical tools are highly needed to identify the material properties responsible for such dramatic failures, as well as to estimate the regional landslides susceptibility (Cascini et al., 2010; Lizárraga et al 2017, 2018). One of the typical examples is the case of shallow landslides, which are frequently triggered by rainfall in pyroclastic soil deposits in Southern Italy. At the REV scale (Representative Element of Volume), the in-situ stress-strain conditions, before and at failure, have been investigated through simple shear device (Cuomo et al., 2015, 2016), which closely approximates the strain-stress paths being the principal (stress/strain) axes free to rotate. Recent developments extended the potential of simple shear to partially saturated soils, with the suction that is usually controlled/measured using the axis translation technique and the tests that can be carried out at constant suction or at constant volume. To numerically elaborate the observed soil behaviours, advanced constitutive models in the simple shear stress space are required, also capable to deal with the hydro-mechanical coupling. However, constitutive models are normally formulated in triaxial conditions, like the Barcelona Basic model (Alonso et al., 2010), the Wheeler-Sivakumar model (Wheeler et al., 1995) and the Modified Pastor-Zienkiewicz model (Pastor et al., 1990). A model extension to simple shear stress states required the mathematical generalization from the space of stress invariants and the manipulations of stress tensor to consider the stress rotation. In this paper, an elastoplastic strain-hardening constitutive model proposed by Buscarnera and di Prisco (2013) intends to numerically reproduce the soil responses under simple shear conditions incorporating experimental evidences.

2. Constitutive model

The constitutive model here used was already published in previous papers (Moscariello et al., 2020, 2021), but hereafter is briefly recalled. The Bishop effective stress (Alonso et al., 2010; Bishop, 1959; Sun et al., 2007) is adopted:

$$\sigma' = \sigma - u_a + S_{re}s \tag{1}$$

where σ is the total stress, u_a is the pore air pressure, s is the suction, S_{re} is the effective degree of saturation following the van Genuchten retention model (1980), defined as:

$$S_{re} = \frac{S_r - S_{\mathrm{res}}}{1.0 - S_{\mathrm{res}}} = [1 + (\alpha_{vg}s)^{n_{vg}}]^{-m_{vg}} \tag{2}$$

where S_{r} is the current degree of saturation, and S_{res} is the residual degree of saturation, and α_{vg}, n_{vg} and $m_{vg} = 1 - 1/n_{vg}$ are shape parameters of the water retention curve. For coarse-grain materials like pyroclastic soils, a frictional relation is often used to define the yielding conditions:

$$f = \tau - \eta_Y \sigma' \tag{3}$$

where η_Y is the stress ratio at yielding, τ is the shear stress, and σ' is the effective normal stress.
A porosity-dependent flow rule is adopted by enhancing the dilatancy function proposed by Lagioia et. al. (1996) with the concept of state parameter ψ (Been et al., 1985; Li et al. 2000), expressed as:

$$D = \frac{\mathrm{d}\varepsilon^p}{\mathrm{d}\gamma^p} = \mu_g\left(M_g^* - \eta\right)\left(\frac{\alpha_g M_g^*}{\eta} + 1\right), M_g^* = M_g \exp\left(m_g \psi\right) \tag{4}$$

where ε and γ are the normal and shear strain with the superscript p representing their plastic parts, μ_g, m_g, and α_g are shape parameters of the dilatancy function and M_g is the critical stress ratio governed by the friction angle φ (i.e., $M_g = \tan\varphi$).
In the dilatancy law, ψ quantifies the distance between current state and the critical state line (CSL) in the n – log(σ') space. This distance is estimated in tems of difference between the current porosity n and the critical state porosity n_{cs}:

$$\psi = n - n_{cs}(1 + bs) \tag{5}$$

where b parameter reflects the effect of the suction on the CSL.
The plastic part of the normal and the shear strain are computed as:

$$\mathrm{d}\varepsilon^p = \Lambda\frac{D}{\sqrt{1+D^2}}, \quad \mathrm{d}\gamma^p = \Lambda\frac{1}{\sqrt{1+D^2}} \tag{6}$$

where Λ is the plastic multiplier derived from the consistency condition. Shear-hardening is captured through the following strain-hardening law:

$$\mathrm{d}\eta_Y = \left(M_p - \eta_Y\right)\frac{1}{\lambda}\mathrm{d}\gamma^p \tag{7}$$

where λ is a hardening constant and it assumes $M_{\mathrm{p}} = M_{\mathrm{g}}$ for simplicity. Finally, the elastic response is modeled through pressure-dependent hypoelasticity with the Young's modulus E and shear modulus G

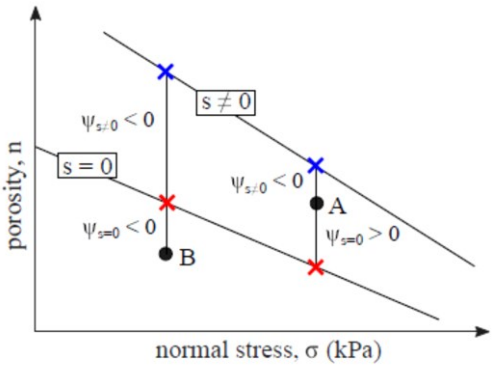

Fig 1. Schematics of the suction-dependent critical state conditions and consequent changes in dilatancy.

expressed as:

$$E = E_r \left(\frac{\sigma'}{\sigma_r}\right)^{n_E}, \quad G = G_r \left(\frac{\sigma'}{\sigma_r}\right)^{n_G} \tag{8}$$

where n_E and n_G are constant power law coefficients; E_r and G_r are the values of the elastic moduli at the reference stress σ_r (normally being 1 kPa).

3. Calibration procedure

Data from triaxial and shear tests performed on remoulded specimens characterized by saturated and unsaturated conditions were used to calibrate the model parameters. Five confidence intervals were identified, based on the statistical distribution of the experimental data, to comply the variation of soil properties associated with SWRC, dilatancy, and shear strength. The intervals correspond to 10% 25%, 50%, 75%, and 95% of probability that a new observation lies within an interval which has as geometric centre axes the curve fit. The complete list of model calibrations's outcomes is given by Moscariello et al. (2021), here the calibration procedure is summarized and the main results presented.

Most of the parameter were calibrated fitting the experimental data and the numerical outputs of the equation detailed in the previous section. The parameters related to the SWRC were calibrated using two wetting tests under simple shear conditions (Fig. 1). Specifically, the SWRCs were extracted considering only the part at constant and low shear strain ($\gamma \approx 0.05$).

The wetting tests adopted were those performed at constant normal stress (30 and 50 kPa) and constant shear stress (34 and 51 kPa), with the suction zeroed at a fixed rate of 0.1 kPa/h.

The elastic parameters (E_r, G_r, n_G and n_E) were obtained by fitting the Eq. 9 with the experimental data obtained from the triaxial tests in drained condition on saturated specimens.

The critical state parameters N_{cs} and λ_{cs} were constrained using the $n - log\sigma'$ plane. However, the confidence intervals couldn't be properly identified because none of the TX, DS and SS tests fully reached the critical state. Therefore, the CSL was approximately evaluated by assuming that the Critical State was reached at large deformations (e.g. for TX tests it was supposed that CSL was reached at axial strain equals to 40%). For the SS tests, the CSL was defined by extrapolating the experimental results for an extra 5% of shear strain. Here, according to previous works (Moscariello et al., 2020), the parameters at critical state are $\lambda_{cs} = 0.031$ and $N_{cs} = 0.78$.

On the other hand, the results obtained in TX, DS and SS tests allow calibrating the parameter M_g, and the dilatancy parameters which are related to the friction angle ϕ. For each test, negligible cohesion was assumed, thus the friction angle was computed as $\tan\phi = \tau/\sigma'$ using the stress values at failure. The confidence levels were identified for ϕ in the $\phi - \sigma'$ plane and an exponential law in that plane was identified:

$$\phi = \phi_0 + c_1 \exp(c_2 \sigma') \tag{9}$$

where ϕ_0, c_1 and c_2 are model constants and σ' is the effective normal stress. M_g was estimated through the outcome of Eq. 9, while The parameters μ_g, α_g and M_g^* were evaluated by fitting the measured dilatancy with the Eq. 4a, while m_g was obtained through the reversal formula of the Eq. 4b, $m_g = \left(\frac{1}{\psi}\right) ln\left(\frac{M_g^*}{M_g}\right)$ (Fig. 2). Finally, the hardening parameter (λ) was determined through a trial-and-error procedure, being 0.06, and then adjusted using the sensitivity analysis and an optimization procedure.

The calibration of the model parameters through experimental data outlined how the variability in soil properties influences the choice of the optimal constitutive parameters. Thus, two further steps were carried out to improve the model performance. A sensitivity analysis based on the confidence levels was carried out estimating the influence of the variation in soil properties on the model predictions. The sensitivity analysis was carried out to investigate the impact of the changes in friction angle, dilatancy and hardening parameters on model performances. The sensitivity analysis outlined that the parameters, which largely influenced the model performance under saturated and unsaturated condition, were those related to shear strength, i.e. the friction angle. The choice of friction angle parameters influenced the model performances in terms of magnitude of the maximum shear stress and normal strain both in saturated and unsaturated condition. The hardening parameter also conditioned the model performances in τ-γ and ε-γ planes, but increasing λ value, the point of maximum curvature of the τ-γ curve was shifted

towards smaller shear strain values. This parameter played a significant role in the wetting tests in simple shear condition. This can be attributed to the low stress strain and stress shear reached upon the shearing stage.

The latter step was carried out through the Optimization Toolbox of Matlab, which uses an iterative procedure, searching a set of input parameters that minimizes the difference between the model outcome and the experimental data. This difference was estimated at selectted shear strain (γ) and in terms of shear stress (τ), normal strain (ε), and degree of saturation (S_r). The error function and its feature were detailed in Moscariello et al. (2021), and here only the results are showed in table 2.

Table 1: List of the test adopted to calibrate the model (data from Bilotta et al., 2005, 2008, Moscariello et al., 2018).

Test type	Condition	Test ID.	s (kPa)	$\sigma - u_a$ (kPa)	σ' (kPa)
Simple Shear	sat	SSP0115	0.0	100.0	100.0
	sat	SSP0315	0.0	76.0	76.0
	sat	SSP0215	0.0	50.5	50.5
	unsat	SSRPSF03a	27.5	97.0	120.1
	unsat	SSRPSF03b	14.7	75.4	138.6
	unsat	SSRPSG23	25.0	50.0	73.0
	unsat	SSRPSG24	25.0	100.0	118.9
Direct Shear	sat	TASNRS21	0.0	9.0	9.0
	sat	TASNRS22	0.0	20.0	20.0
	sat	TASNRS23	0.0	29.0	29.0
	sat	TASNRS25	0.0	39.0	39.0
	sat	TASNRS24	0.0	54.0	54.0
	sat	TASNRS26	0.0	59.0	59.0
	sat	TASNRS29	0.0	69.0	69.0
	sat	TASNRS28	0.0	79.0	79.0
	sat	TASNRS27	0.0	104.0	104.0
	sat	TASNRS31	0.0	133.0	133.0
	sat	TASNRS32	0.0	135.0	135.0
	unsat	TAL0608	25.0	73.4	73.4
	unsat	TAL0808	45.0	50.0	50.0
	unsat	TAL1008	60.0	89.3	89.3
Test type	Condition	Test ID.	s (kPa)	$p - u_a$ (kPa)	p' (kPa)
Triaxial	sat	BIS2206	0.0	100.0	100.0
	sat	BIS2306	0.0	100.0	100.0
	sat	BIS2406	0.0	100.0	100.0
	sat	BIS2606	0.0	50.0	50.0
	sat	BIS2706	0.0	200.0	200.0
	sat	BIS2806	0.0	30.0	30.0
	sat	BIS2906	0.0	30.0	30.0

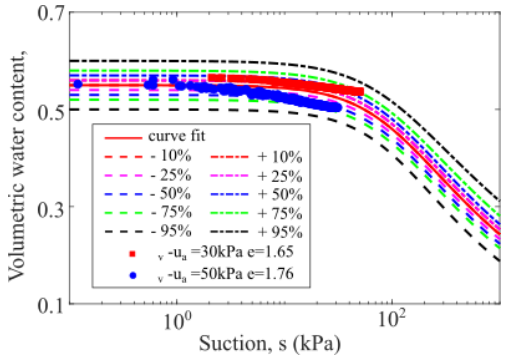

Fig 2. Calibration of the Soil Water Retention curves interpolated using van Genuchten retention model. Note -/+ indicates the lower/upper boundary of the studied confidence level.

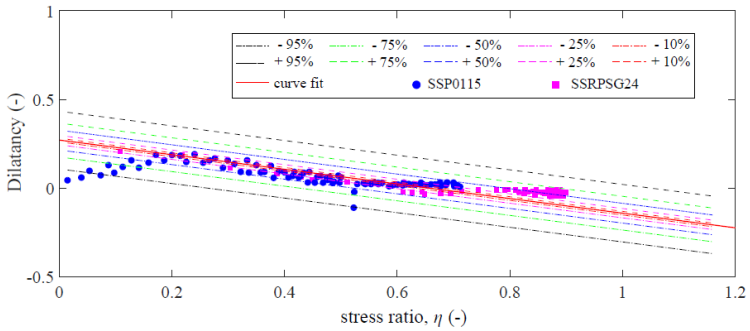

Fig 3. Calibration of dilatancy parameters through two direct shear tests performed on saturated (SSP0115) and unsaturated (SSRPSG24) specimens (Moscariello et al., under review).

Table 2: Parameter variations obtained through sensitivity analyses and optimization procedure.

Category	Symbols	Unit	-
Plasticity	α_g	-	0.0
	m_g	-	0.994
	μ_g	-	0.22
	b	1/kPa	0.02
	λ	-	0.06
shear strength	ϕ_0	°	35.67
	c_1	-	15.40
	c_2	1/kPa	0.022

The optimization procedure allowed obtaining a single set of constitutive parameters, which provided satisfactory simulation of the hydro-mechanical soil response in simple shear condition under several saturation condition and failure mechanisms.

4. Model performances

Both the simple shear saturated and unsaturated tests, and the simple shear wetting tests were simulated using the unified optimized parameters reported in Table 2.
The general agreement between the experimental results and the constitutive modelling is discussed with reference to τ-γ and ε-γ planes for simple shear saturated and unsaturated tests, and with reference to γ-s and ε-s planes for the simple shear wetting tests.

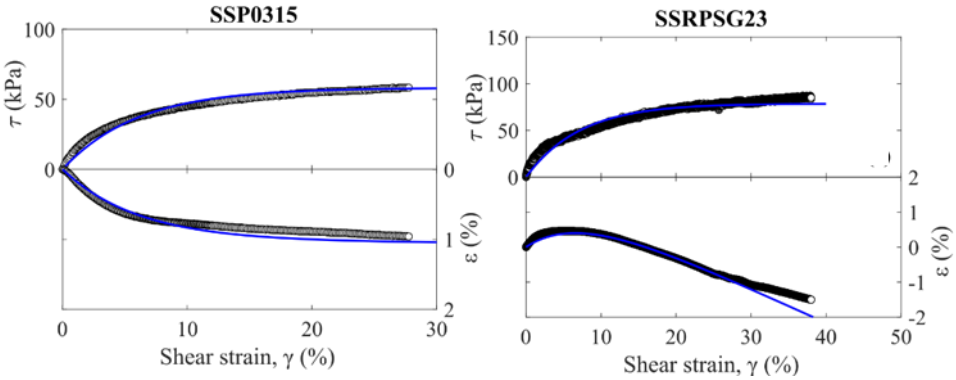

Fig 4. Comparison between measurements and numerical results of a simple shear test in saturated and unsaturated condition obtained using the calibrated parameter set proposed in Table 2.

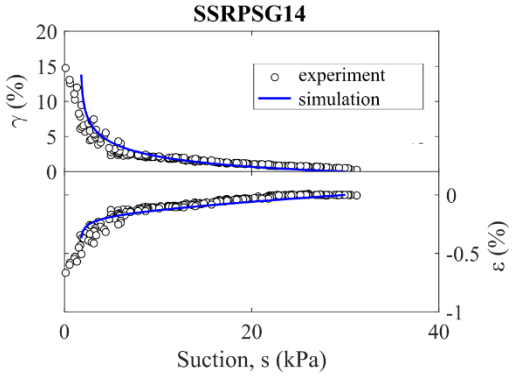

Fig 5. Comparison between measurements and numerical results of wetting test in simple shear condition obtained using the calibrated parameter set proposed in Table 2.

The best numerical simulations in both the planes simultaneously considered were obtained for SSP0315 (saturated), and SSRPSG14 (wetting test). The trend of volumetric behaviour was also captured for SSRPSG23 (Fig. 4), but slight differences can be observed at shear strain higher than 30%. Some differences were also observed at low shear strain for SSP0315 and SSRPSG23 tests (Fig.4 and 5).

5. Conclusions

The simple shear response of air-fall volcanic (pyroclastic) soils under both saturated and unsaturated conditions was interpreted through an elastoplastic constitutive model with hydraulic-hardening and porosity-dependent critical state. The calibration was performed using a large data set of experimental results, i.e. triaxial test, direct and simple shear tests in saturated and unsaturated regime. The model performances were improved through a sensitivity analysis and an optimization procedure. The proposed procedure allowed a single set of constitutive parameters to be obtained, which provided satisfactory simulation of the hydro-mechanical soil response in simple shear condition under several saturation condition and failure mechanisms. However, the model was calibrated and validated on three failure mechanisms but for the same soil. Thus, further investigations could enlarge the application of the calibration and optimization proposed procedure also to other soils.

Bibliografia

Alonso, E. E., Pereira, J. M., Vaunat, J., & Olivella, S. (2010). A microstructurally based effective stress for unsaturated soils. *Géotechnique*, *60*(12), 913-925.

Bishop, A. W. 1959. The principle of effective stress. *Teknisk ukeblad*, *39*, 859-863.
Cascini, L., Cuomo, S., Pastor, M., & Sorbino, G. (2010). Modeling of rainfall-induced shallow landslides of the flow-type. *Journal of Geotechnical and Geoenvironmental Engineering*, *136*(1), 85-98.
Cuomo, S., Foresta, V., & Moscariello, M. (2016). Shear strength of a pyroclastic soil measured in different testing devices.
Lizárraga, J. J., & Buscarnera, G. (2018). Safety factors to detect flowslides and slips in unsaturated shallow slopes. *Géotechnique*, 68(5), 442-450.
Lizárraga, J. J., Frattini, P., Crosta, G. B., & Buscarnera, G. (2017). Regional-scale modelling of shallow landslides with different initiation mechanisms: Sliding versus liquefaction. *Engineering geology*, *228*, 346-356.

Moscariello, M., Chen, Y., Cuomo, S., & Buscarnera, G. (under review) Data-driven calibration of a constitutive model for volcanic sands under simple shear conditions

Moscariello, M., Chen, Y., Cuomo, S., & Buscarnera, G. (2020). Modelling of simple shear tests on volcanic unsaturated sands. In *E3S Web of Conferences* (Vol. 195, p. 02021). EDP Sciences.
Pastor, M., Zienkiewicz, O. C., & Chan, A. H. C. (1990). Generalized plasticity and the modelling of soil behaviour. *International Journal for Numerical and Analytical Methods in Geomechanics*, *14*(3), 151-190.